Phase contrast wavefront sensing for adaptive optics

E. E. Bloemhof and J. K. Wallace
Jet Propulsion Laboratory, California Institute of Technology,
Pasadena, CA USA 91109

ABSTRACT

Most ground-based adaptive optics systems use one of a small number of wavefront sensor technologies, notably (for relatively high-order systems) the Shack-Hartmann sensor, which provides local measurements of the phase slope (first derivative) at a number of regularly-spaced points across the telescope pupil. The curvature sensor, with response proportional to the second derivative of the phase, is also sometimes used, but has undesirable noise propagation properties during wavefront reconstruction as the number of actuators becomes large. It is interesting to consider the use for astronomical adaptive optics of the "phase contrast" technique, originally developed for microscopy by Zernike to allow convenient viewing of phase objects. In this technique, the wavefront sensor provides a direct measurement of the local value of phase in each subaperture of the pupil. This approach has some obvious disadvantages compared to Shack-Hartmann wavefront sensing, but has some less obvious but substantial advantages as well. Here we evaluate the relative merits in a practical ground-based adaptive optics system.

Keywords: adaptive optics, wavefront sensing, phase contrast

1. INTRODUCTION: PHASE CONTRAST THEORY OF OPERATION

The Zernike phase contrast technique is well known as a means of enhancing imaging in microscopy[1], where it can convert phase variations across a transparent, otherwise invisible object into intensity variations. This capability is particularly useful in allowing biological tissue samples to be seen and their internal structures studied, though the intensity of light transmitted through these samples is not much different than that through the surrounding medium. The basic characteristic of determining relative optical phase thicknesses suggests that the technique might be more generally applicable for wavefront sensing. At Palomar, the phase contrast technique has been used at a relatively low bandwidth, to calibrate non-common-path phase errors in the PALAO adaptive optics (AO) system[2]. In the current paper, we continue and extend our study of the feasibility of phase contrast as a real-time wavefront sensor in adaptive optics systems[3,4], measuring the phase variations across the telescope pupil that are the basic quantity to be corrected, at the high frame rates needed to keep up with atmospheric phase fluctuations.

The basic experimental element of the phase-contrast wavefront sensor (Figure 1) is a phase-shifting focal-plane filter. This element provides a relative phase shift of $\pi/2$ between the general field and an on-axis spot roughly λ/D in diameter, which is the diffraction-limited imaging scale for monochromatic observations at wavelength λ on a telescope of diameter D. (Techniques for extending operation to broad spectral bandwidths, suitable for astronomy, have been presented[4]. Achromatic phase shifts can be produced through multi-layer films, and are of interest in the novel four quadrant phase mask [FQPM] coronagraph[5]. Achromatization of the focal-plane filter spot diameter can effectively be accomplished by an arrangement of lenses: see Section 4) As will be shown below, this arrangement will produce an intensity distribution in a reimaged pupil that has a component directly proportional to phase Φ, for small Φ.

The theory of operation of the phase-contrast wavefront sensor can be presented simply in terms of Fourier optics[6,7]. The telescope is described by an aperture function $A(\xi,\eta)$ of spatial coordinates ξ and η on the pupil, typically an annular shape resulting from a primary mirror obscured by a secondary mirror. If the aperture is not apodized, the aperture function will assume only the values 1 and 0, depending on where the pupil admits light and does not. (Atmospheric scintillation, another source of amplitude fluctuations, is not considered here). Light from a distant unresolved guide star produces optical fields across the telescope aperture of diameter D that are described by a two-dimensional phase function $\Phi(\xi,\eta)$ of the same support as the aperture function. (If there were no atmospheric turbulence these fields would very nearly be plane waves, described by $\Phi=0$.)

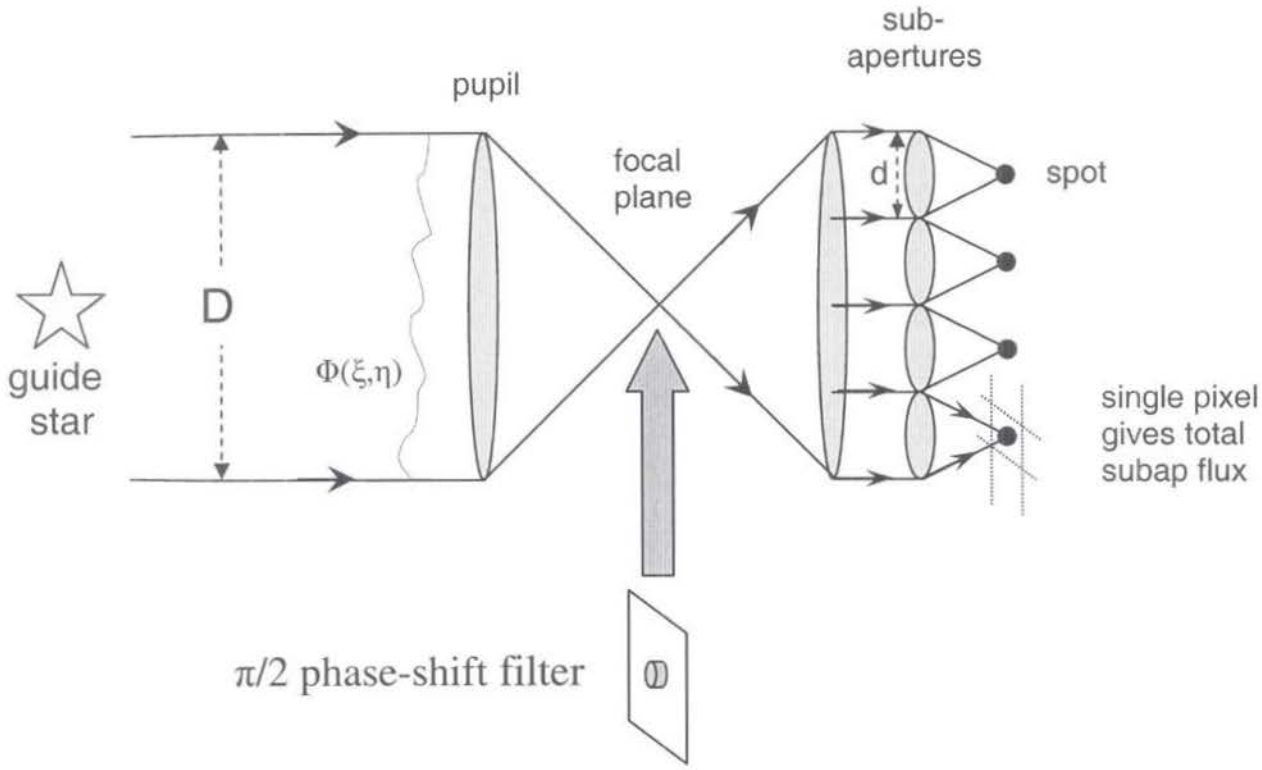

Figure 1 – Optical layout of a phase-contrast wavefront sensor. The filter, roughly λ/D in diameter for monochromatic light, and introducing a phase shift of $\pi/2$ relative to rays not hitting the filter, is inserted in an intermediate focal plane. Intensity across a reimaged pupil has a component proportional to the phase Φ of the incident wavefront from the unresolved guide star.

The focal-plane optical fields are related to those in the pupil plane by Fourier transformation:

$$focal-plane \;\; field(x,y) = F.T.\left[A(\xi,\eta)\exp\{i\phi(\xi,\eta)\}\right] \tag{1}$$

and the image intensity in either plane may be found by taking the squared modulus of the field, $|\ldots|^2$. If the incident wavefront is flat, the image with $\Phi=0$ reduces to the telescope point-spread-function (PSF), $|F.T.\{A(\xi,\eta)\}|^2$. More typically on ground-based telescopes, the turbulent atmosphere induces strong phase distortions whose transverse coherence scale is r_0, roughly tens of cm in the visible and near-infrared. These disperse the light from the star into a halo of speckles moving within a region roughly λ/r_0 in diameter, rather than the diffraction-limited diameter of the PSF, λ/D. The strength of atmospheric turbulence is characterized by the Strehl ratio S, related to the mean-square phase disturbance of the wavefront across the pupil by $S = 1-\langle\Phi^2\rangle$, for small values of that disturbance. Both the strength of turbulence and its characteristic spatial scale(s) are important characteristics controlling speckle behavior.

In the limit of small phase Φ, or equivalently of high Strehl ratio S, the phase exponential in the pupil-plane optical field may be expanded as $1+i\Phi$, indicating that the phase-contrast signal proportional to Φ is initially $\pi/2$ out of phase with a stronger component not affected by the phase perturbations. In more detail, the pupil-plane field in this small-phase approximation becomes:

$$pupil\ field(\xi,\eta) = A(\xi,\eta)\exp\{i\phi(\xi,\eta)\} \approx A(\xi,\eta)\{1+i\phi(\xi,\eta)\} \qquad (2)$$

That stronger component is uniform over the pupil, producing a bright diffraction-limited image in the focal plane of width ~ λ/D; the weaker term in Φ carrying the phase-contrast information of interest is diffracted off-axis from the PSF. Hence only the strong "undiffracted" central rays intercept the phase-contrast focal-plane filter and are phase-shifted by $\pi/2$, bringing the two optical field components into phase with each other. In a subsequent reimaged pupil plane, each component has the same spatial distribution it had over the original pupil plane, but now squaring the modulus of the total field strength and retaining the leading-order term in Φ shows the intensity for small Φ is proportional to $1\pm2\Phi$. This implies a "phase-contrast signal" map $2\Phi(\xi,\eta)$ superimposed on a uniform intensity across the entire pupil. (Strictly speaking, the phase-contrast sensor need not be operated only in this linear regime[8].)

The theoretical fidelity of the reimaged pupil intensity to phase over the original pupil is illustrated in Figure 2, a numerical simulation of a phase-contrast wavefront sensor at moderately high and very high Strehl (S= 0.7 and 0.99, respectively). At higher Strehl the fidelity is greater, but the signal is masked by a relatively larger uniform background intensity, with proportionately less light in the phase-contrast signal channel, 2Φ.

Phase-Contrast WFS Signal (contours)
overlaid on input phase function (grayscale)

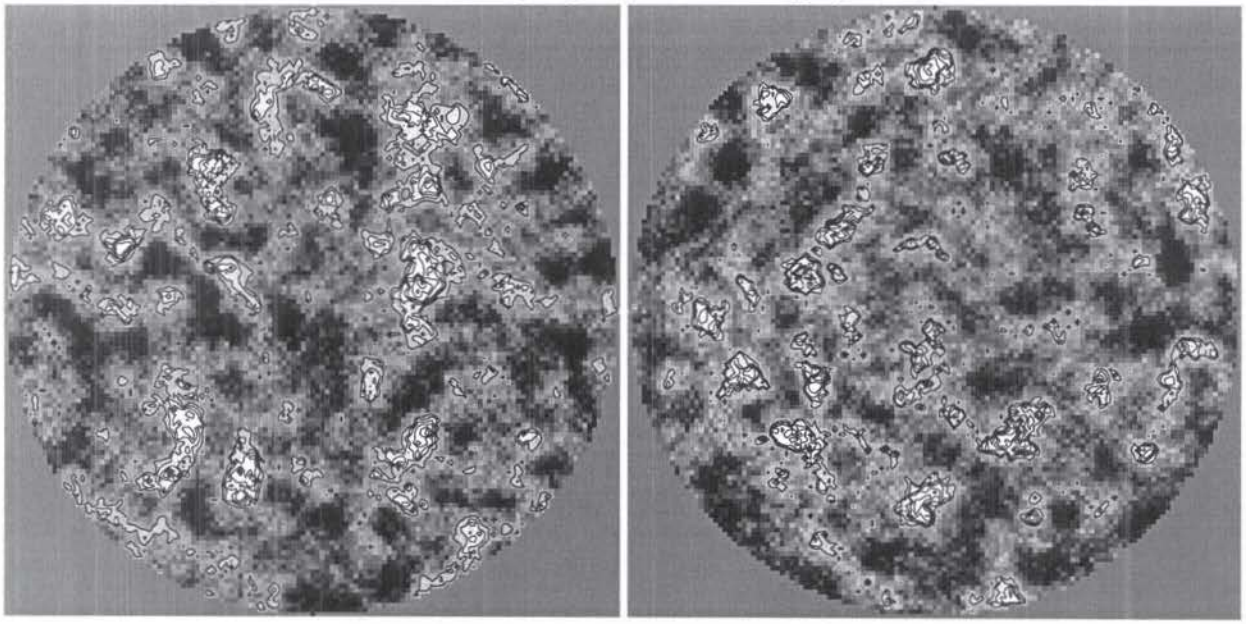

S = 0.99 **S = 0.70**

Figure 2 – Numerical simulation of the fidelity of signals from a phase-contrast wavefront sensor. Each grayscale image is a random phase screen incident on the telescope pupil, with Strehl ratios S = 0.99 (left) and 0.70 (right). Light regions are larger phase, black is zero phase, and the scales are arbitrary and different between the two plots. Each phase screen has D/a~16: i.e., the linear spatial density of coherent cells per pupil diameter is about 16. Overlaid contour plots in each case trace the strength of the phase-contrast signal. The correlation is clearly good in this range of correction parameters. For clarity, only a few of the highest contours, arbitrarily chosen, have been drawn.

2. CURRENT ASTRONOMICAL WAVEFRONT SENSORS: THE SHACK-HARTMANN

Some valuable scientific work has been done with curvature sensing wavefront sensors for astronomical adaptive optics system. These systems are particularly simple, so they were implemented quickly and provided some of the earliest astrophysical results[9]. They produce an error signal proportional to the local curvature (second spatial derivative) of the wavefront by comparing images taken in rapid succession at two focal positions, one above and one below nominal telescope focus. Curvature wavefront sensors have often been coupled to bimorph deformable mirrors, which directly produce a local phase curvature that is proportional to drive voltage. Although sensitivity of individual local wavefront measurements in a curvature wavefront sensor is competitive with alternative approaches[10], a disadvantage of curvature sensors becomes apparent when the number of control actuators in the AO system becomes very large. In that case, the error propagation during wavefront reconstruction is unfavorable compared to that of the Shack-Hartmann wavefront sensor, the sensor chosen for most astronomical AO systems, whose error signals are proportional to the first spatial derivative, or slope, of phase (also called tip/tilt). (Quantitatively, the curvature wavefront sensor produces a reconstructed error that increases in rough proportion to the total number of actuators/wavefront-sensor elements, while the Shack-Hartmann has a slow logarithmic dependence on that number[11].) Since high correction will involve large deformable mirror actuator counts, we will take the Shack-Hartmann wavefront sensor to be representative of the current state of the art for large astronomical AO systems.

A schematic of a Shack-Hartmann wavefront sensor is shown in Figure 3. This is the sensor used in PALAO, the Palomar Adaptive Optics system[12,13], and hence of most interest to us.

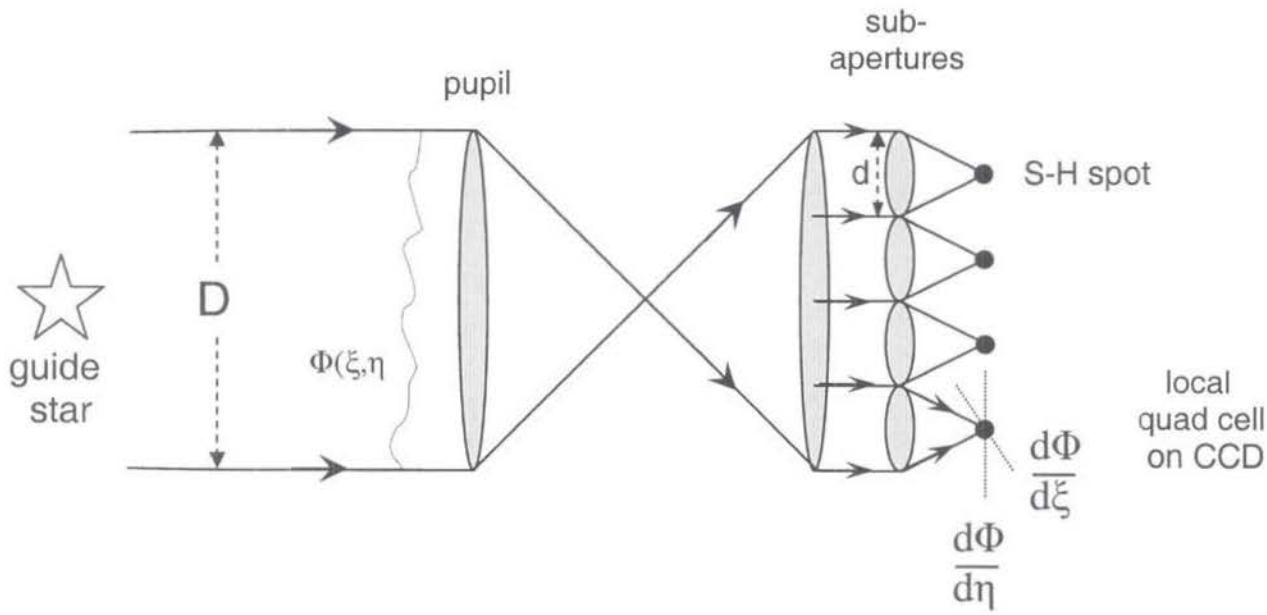

Figure 3 – Schematic of the Shack-Hartmann wavefront sensor, the type most commonly used in astronomical adaptive optics. A reimaged pupil is divided into subapertures with size comparable to r_0, the transverse coherence scale of atmospheric turbulence. Light from each subaperture is focused by an element in a lenslet array onto a group of four CCD camera pixels that act as a quadcell. Two-dimensional spot deflection is proportional to wavefront tip/tilt (phase gradients) on the telescope pupil.

3. PERFORMANCE COMPARISON BETWEEN PHASE-CONTRAST AND SHACK-HARTMANN REAL-TIME WAVEFRONT SENSORS

a) Sensitivity of Single-Subaperture Measurement: Shack-Hartmann WFS

The limiting sensitivity in a single one-dimensional measurement of wavefront tilt with a Shack-Hartmann wavefront sensor, for an unresolved guide star and no gap between quadcell pixels, is given by[10]

$$\Delta\theta_x = \frac{3\pi}{16}\frac{\lambda}{d}\frac{1}{SNR} \tag{3}$$

Here d is the diameter of a wavefront sensor subaperture mapped onto the entrance pupil (telescope primary) and SNR is the signal-to-noise ratio of the subaperture light level measurement, counting the total light detected in all four quadrants of the quadcell. This expression assumes that subaperture wavefronts are flat, i.e., that d is substantially smaller than r_0. Equation (3) can be converted to phase sensitivity by simple geometry: when a measurement of wavefront tilt at the limit of sensitivity is made in a single subaperture, phases at the corners of that subaperture are different by

$$\Delta\Phi_x = (\Delta\theta_x)d\frac{2\pi}{\lambda} = \frac{6\pi^2}{16}\frac{1}{SNR} \sim \frac{6\pi^2}{16}\frac{1}{\sqrt{n}} \sim \frac{3.7}{\sqrt{n}} \tag{4}$$

In order to simplify the comparison between wavefront sensors, we have made in the last two expressions the rather gross assumption that one may neglect noise sources other than the familiar $\sqrt{n}$ photon noise on a detected photon count of n per subaperture and per integration time or cycle time of the wavefront sensor. These expressions may easily be generalized to include other detector noise sources, and in fact a more detailed examination of some detector-noise issues would favor the phase-contrast wavefront sensor: for example, reading out four pixels of the WFS CCD camera to make a single subaperture measurement in the Shack-Hartmann causes commensurately higher read noise. Note also that Equation (4) refers to a one-axis phase slope measurement; the two-axis case would be noisier by $\sqrt{2}$.

b) Sensitivity of Single-Subaperture Measurement: Phase-Contrast WFS

The corresponding sensitivity calculation for the phase-contrast wavefront sensor requires no conversion for geometry. In this case, the portion of intensity in the phase-contrast signal channel, 2Φ, directly gives the phase, rather than the phase slope; the total intensity is proportional to $1+2\varphi$, including the uniform background level due to the undiffracted rays. The average intensity is n detected photons per subaperture and per integration time, found by the usual considerations of guide-star flux, telescope aperture, and AO system speed; if for simplicity of presentation we again consider only photon noise, the average subaperture noise level is $\sqrt{n}$. The phase sensitivity is the phase that gives a phase-contrast wavefront-sensor signal $2\Phi n$ matching this noise level:

$$\Delta\Phi \sim \frac{1}{2\sqrt{n}} \tag{5}$$

(we neglect the difference between 1 and $1\pm2\Phi$ as Φ, presumed small, ranges over positive and negative values). Comparing Equations (4) and (5), the phase-contrast wavefront sensor is more sensitive in a single-subaperture phase measurement by a substantial factor (~7.4) in this idealized scenario. An important modification to this simple picture is that the phase-contrast wavefront sensor will register a false signal when atmospheric scintillation causes the total subaperture intensity to fluctuate; this may typically be 10% or so of the nominal level. However, this would imply a phase noise floor of only about 0.05 radians, corresponding to a Strehl ratio of over 99%, so is unlikely to be a significant restriction on AO system operation. (The same point can be seen in Figure 4, which also shows that the fraction of intensity in the phase-contrast channel, even normalized pessimistically, is substantial up to fairly high Strehl.) The effects of scintillation might also be mitigated during reconstruction if the atmospheric phase Φ is sufficiently continuous that correlations between neighboring subapertures effectively provide averaging of the signal.

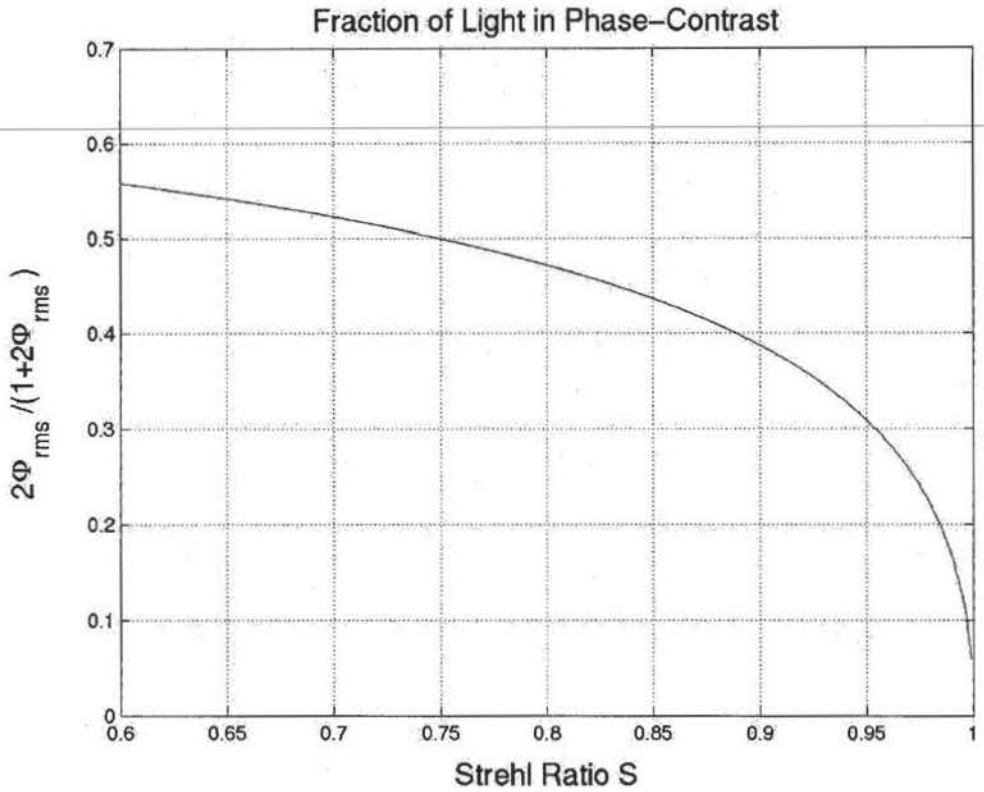

Figure 4 – Amount of guide-star light appearing in phase contrast (2Φ), as a fraction of the total guide-star light, ($1+2\Phi$), at an rms residual phase level Φ corresponding to a given Strehl ratio via the high-Strehl approximation, $\Phi=\sqrt{(1-S)}$. Even at very high performance levels, a substantial fraction of guide-star light in the phase-contrast wavefront sensor contains useful information about the wavefront.

c) Error Propagation During Wavefront Reconstruction:

After phases or phase gradients are measured with good sensitivity at an array of positions over the pupil, it remains to accurately derive an overall wavefront. This "reconstruction" step has been studied, and error propagation properties determined. If the mean-square error in the one-axis, single-subaperture phase gradient measurement of an *NxN* Shack-Hartmann in the standard ("Fried") geometry is $\sigma^2_{1\text{-axis}}$, then the mean-square error in the reconstructed wavefront is[14]

$$\left\langle (\delta\,\Phi)^2 \right\rangle \approx 0.6558\left[1+0.2444\ln\left(N^2\right)\right]\sigma^2_{1-axis} \qquad (6)$$

For N=16 (e.g. Palomar AO), the numerical prefactor is 1.54; it would be 2.13 for an "extreme" AO system with N=100. As mentioned earlier, this is substantially less than the error that propagates through a curvature sensor when N is large, and the difference is qualitatively understood in terms of the greater spatial correlation of wavefront slope compared to wavefront curvature. This redundancy is exploited during reconstruction to give more benign error propagation[10,11]. Presumably, direct phase measurements are more correlated still. A useful comparison may be made with the analysis by Hudgin[15] of a wavefront sensor producing estimates of phase differences between adjacent subapertures:

$$\left\langle (\delta\,\Phi)^2 \right\rangle \approx \left[0.561+0.103\ln(N)\right]\sigma^2_{1-msmt} \qquad (7)$$

The numerical prefactor here is 0.85 for N=16, and 1.04 for N=100. One would generally expect the prefactor to be ~1.0 for direct phase measurements in wavefront sensor cells separated by r_0, which should possess independent phase values,

but it could be less if continuity of phase between adjacent subapertures permitted some degree of averaging. For either estimate, it appears likely that the phase-contrast wavefront sensor may enjoy an advantage over the Shack-Hartmann in noise propagation during wavefront reconstruction, by a factor of 1.5 to 2 in mean-square wavefront.

d) Speed of Computation:

One function of wavefront reconstruction in a typical AO system is conversion of wavefront slope measurements from a Shack-Hartmann sensor into the wavefront error signals needed by piston-type deformable-mirror (DM) actuators. The fact that the phase-contrast wavefront sensor directly measures phase values, rather than higher derivatives of the phase function, makes reconstruction almost unnecessary. This natural match between wavefront sensor and deformable mirror can simplify and reduce the computational load, speeding up the response of the AO control loop. Latency in the real-time computation can be a limiting factor in the performance of AO systems. Full matrix reconstruction for an NxN Shack-Hartmann requires multiplying an N^2x2N^2 control matrix by a $2N^2$x1 column vector of x- and y-gradients of the pupil phase to obtain N^2 updated DM actuator positions, involving a total of $\sim 2N^4$ multiplication and additions. In the phase contrast case, full reconstruction would nominally imply multiplying a square N^2xN^2 control matrix by an N^2x1 column vector of pupil phases, immediately implying half as many mathematical operations.

But the computational gains are even greater. The Shack-Hartmann control matrix is the pseudo-inverse of a *rectangular* influence matrix that maps a commanded wavefront (DM actuator deflections) into a set of responses from the wavefront sensor (phase gradients). This influence matrix is relatively sparse: if the influence function of individual DM actuators is approximated as a δ-function (i.e., moving an actuator does not affect the surface at the positions of neighboring actuators), the influence matrix consists of 4 non-zero diagonals representing the 4 DM actuators that surround any wavefront sensor subaperture in the Fried geometry and determine its gradients. The pseudo-inverse of the influence matrix, the control matrix, is generally fully populated; but if it is approximately sparse, the computational load for its inversion can be reduced from $2N^4$ to $2d^2N^2$, where d is the size of the local influence region[16].

The phase-contrast influence matrix is square, not rectangular, and by its nature is very close to diagonal, so its inverse is close to diagonal also. Sparse-matrix techniques should therefore be quite effective in producing high computational efficiency. When the influence function intrinsic to the DM actuators themselves is convolved with either the 4 diagonals of the Shack-Hartmann or the single diagonal of the phase-contrast sensor, the net influence matrix is more closely diagonal in the phase contrast case. The substantial reduction in computational load described here implies a significant increase in control bandwidth for comparable computing resources. This will give improved performance for the phase-contrast wavefront sensor, and quantitatively expresses the advantage of matching a wavefront sensor that directly measures phase piston to deformable mirrors that produces phase pistons in response to drive signals.

e) Additional Advantages:

The phase-contrast wavefront sensor should enjoy a number of other advantages over the Shack-Hartmann. It should suffer a smaller loss of sensitivity when the guide star is partially resolved, in which circumstance a quadcell is seriously compromised. The Shack-Hartmann, when coupled to a square array of DM actuators in the "Fried" geometry, produces a characteristic pattern of image artifacts known as "waffle mode", intensity ghosts arranged symmetrically in a square about the PSF peak. This image defect results from the fact that the Shack-Hartmann cannot sense pupil-plane phase patterns corresponding to a checkerboard of actuators alternating between two offset levels; this unsensed mode and its corresponding image-plane artifacts then tend to grow in a random-walk fashion if no special actions are taken to monitor them. No comparable defects could be incurred when phase is sensed directly by the phase-contrast wavefront sensor, because there are no pupil-plane phase modes (except for overall piston) that are not sensed by the subaperture arrangement. Hence the phase-contrast wavefront sensor enjoys a cosmetic advantage and small formal advantage in wavefront error over the standard Shack-Hartmann configuration. Another advantage of the phase-contrast wavefront sensor is its immunity to centroid anisoplanatism errors[17], though this is normally a small effect. The error is related to the fact that Zernike phase functions over a pupil or subaperture are orthogonal, but their corresponding image-plane intensities are not. So, for example, coma is orthogonal to true tip/tilt ("Z-tilt", or Zernike tilt), but has an asymmetric image intensity distribution that contributes a non-vanishing (and erroneous) spot displacement in a Shack-Hartmann quadcell that measures "G-tilt", or gradient tilt.

4. ACHROMATIZATION OF THE PHASE-CONTRAST WFS

In a wavefront sensor for astronomical use, it will always be critical to maximize sensitivity by offering response to the broadest possible wavelength band of guide-star light. A Shack-Hartmann sensor operated in a regime that is linear for all wavelengths in the band is intrinsically broad-band, giving a quadcell spot deflection that is the same for all wavelengths for a given subaperture tip/tilt. It is less obvious, but the phase-contrast wavefront sensor may also be made achromatic. To do so requires two tasks: the excess phase thickness of the central spot in the focal-plane filter must be achromatized, and made equal to $\pi/2$, and the diameter of that spot must be made to be roughly λ/D, where D is the diameter of the telescope aperture, for all wavelengths λ in the band. The former requirement fixes the magnitude of the phase shift necessary to bring into step the undiffracted wave and the higher-order waves that carry information about the phase over the pupil plane; the latter requirement relates to the spatial extent of the undiffracted wave. Both of these steps appear feasible, though each involves a relatively challenging development effort. The first task involves precise thin-film design and fabrication, while the second may be achieved with external optics.

Achromatization of the phase shift involves design principles akin to those being pursued in the novel four quadrant phase mask (FQPM) coronagraph, although in that case an achromatic phase shift of π is required. The $\pi/2$ phase shift appears more difficult, and cannot take advantage of the "natural" π phase shift that occurs on reflection from a denser medium. The thin-film design techniques are familiar from multi-layer films, such as anti-reflection coatings. Resolution requirements for fabricating the phase-shifting filter, of diameter about $\lambda/D \sim 25$ μm at visible wavelengths, are easily within the capabilities of linewidth definition for optical photolithography. Excellent high- and low-index pairs with good adhesion, such as TiO_2 (n = 2.3) and SiO_2 (n = 1.5), are available to act as the building blocks for engineering thin films of tailored properties. The schematic approach diagrammed in Figure 1 is not literally acceptable for an achromatic phase-shifting filter, because the phase equivalent of the air column surrounding the central spot is highly chromatic. Thus, in addition to a broad-band design for the central spot, a surrounding medium with appropriate broad-band response is required so that the differential phase shift is an achromatic $\pi/2$.

Achromatization of the transverse size of the focal plane phase-shifting spot, to match $\sim\lambda/D$ over the wavelength passband of interest, may be achieved through optics surrounding the focal-plane phase-shifting filter that provide a compensating, achromatic transverse magnification. Simple designs for lens systems giving wavelength-dependent magnification have been proposed by Wynne[18] and by Roddier et al.[19] The performance of an achromatic corrector is graphed by Wynne, who sought to compensate the chromatic dispersion of speckle patterns in images. Over 400 nm to 700 nm, the normal wavelength-dependent variation of image height in the focal plane would be 700/400 = 1.75. The correcting lens optics reduce this linear variation to a shallow parabolic dependence on wavelength; magnification is roughly the same at each end of the wavelength band, and drops only about 7% in the middle. Such optics positioned around the phase-shifting focal-plane filter would match the scale of the phase-shifting spot to the lowest spatial order of light to good accuracy over a broad range of wavelengths, allowing, in conjunction with the achromatic phase shift described in the previous paragraph, broad-band operation of the phase-contrast wavefront sensor.

5. PRACTICAL IMPLEMENTATION: SYSTEM DESIGN CONSIDERATIONS FOR AN ASTRONOMICAL PHASE-CONTRAST WAVEFRONT SENSOR

Some initial concepts for implementing a phase-contrast wavefront sensor in a practical adaptive optics system have been considered. Locking such a system from initially uncontrolled atmospheric turbulence appears challenging: if one initially selects a subregion of the pupil over which the phase excursions are small enough to give linear operation, the transverse dimension of the focal-plane phase-shifting filter would have to adjust as the lock progressed, narrowing from λ/d to λ/D. An interesting alternative is to "bootstrap" a phase-contrast wavefront sensor onto a Shack-Hartmann "on the fly", when the Shack-Hartmann has already achieved a correction sufficient to enable the phase-contrast sensor to operate over the full pupil. It appears that this approach is feasible from the viewpoint of basic system engineering. For example, the layout of PALAO, the Palomar Adaptive Optics system (Figure 5) appears amenable to accommodating a phase-contrast wavefront sensor with only minor modifications.

A promising concept involves fabricating the phase-shifting spot on the field stop (FS), positioning it slightly out of the focused beam from the guide star during Shack-Hartmann observations. Shifting to phase-contrast mode would involve

a commanded tip-tilt to bring the focused beam onto the spot, which would simultaneously move the image in each subaperture off the four-pixel quadcell vertex and onto a single pixel, as required. The geometry of the phase-contrast wavefront sensor is not ideal in this scheme, as subapertures are not located directly underneath DM actuators. It is expected that adaptive lock could still be captured with improved error propagation during wavefront reconstruction because the pupil-plane phase should have sufficient spatial continuity; if so, the relative positioning of DM actuators and wavefront sensor pupil could be adjusted to optimize system performance after lock is captured, or a more complicated reconstructor involving interpolation of phases could be used initially.

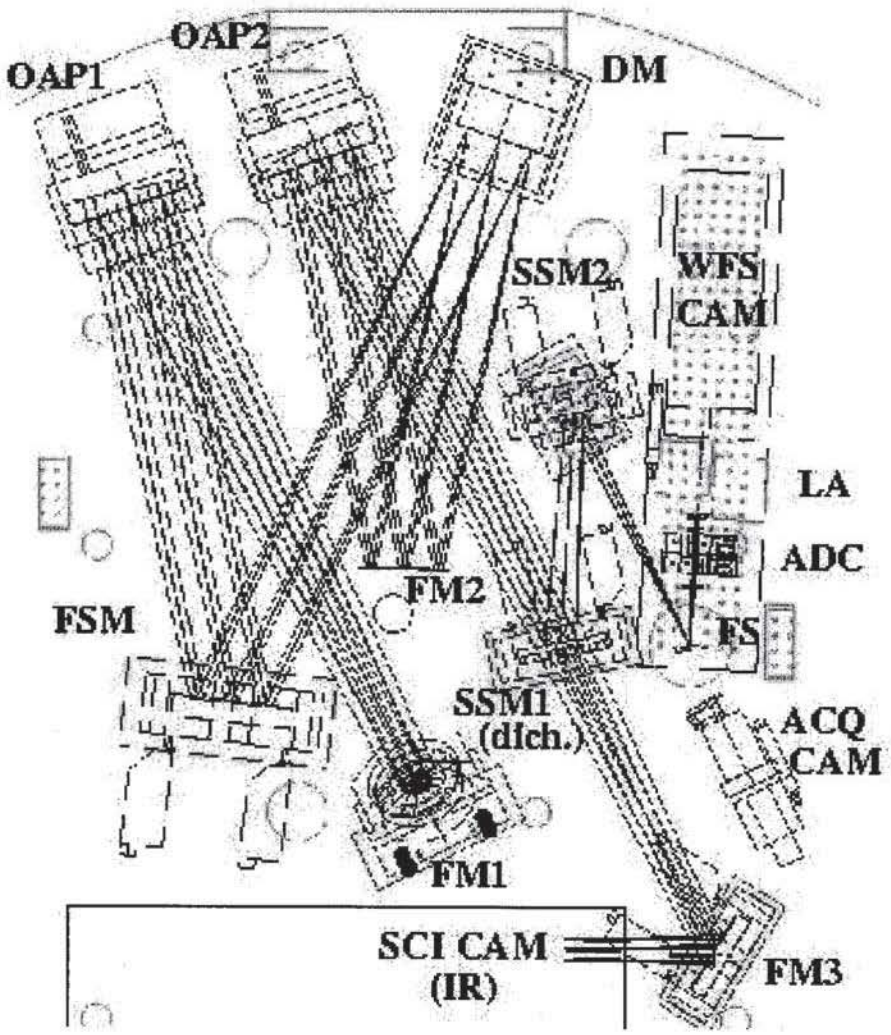

Figure 5 – Optical layout of PALAO, the Palomar Adaptive Optics system, a high-order system that uses a Shack-Hartmann wavefront sensor. Light from the telescope is injected, from out of the plane of this drawing, at FM1. Fast tip-tilt correction is applied by FSM; higher-order correction is provided by DM. The science camera operates in the near-infrared; visible light is sent to the wavefront sensor via steering mirrors SSM1 (a dichroic) and SSM2. The reflective field stop (FS), a 4 arcsec x 4 arcsec metallization on an otherwise transparent substrate, directs the guide-star light through the Shack-Hartmann lenslet array (LA) and onto the CCD camera (WFS CAM).

PALAO correction can be as high as S=0.7, which should be high enough to allow the wavefront sensor transition described here. An interesting experiment may go on-line in a year or two to field a four quadrant phase mask (FQPM) on an unobscured subregion of the Palomar primary, and the higher DM actuator density thus obtained should allow S=0.9 under Shack-Hartmann operation. In any event, the auxiliary optics and phase-shifting spot (positioned clear of the beam until needed) that would be used for a phase-contrast mode do not appear to interfere with normal operation of the Shack-Hartmann wavefront sensor.

6. CONCLUSIONS

We have presented a general examination of the practicality of using the phase contrast technique as a wavefront sensor in astronomical adaptive optics systems. In comparisons with the Shack-Hartmann sensors now commonly used, the phase contrast approach appears promising for extending an initially good correction into regimes of much higher performance. There is some loss of signal from the useful phase-contrast channel that reduces the signal as correction is improved, but this does not appear serious even beyond S~0.7 (Figure 4). There will be substantial advantages in noise propagation during reconstruction, and in computing speed, owing to the better match of the phase-contrast wavefront sensor to piston-type DM actuators. The detailed steps needed to achieve very broad wavelength coverage do not seem insurmountable, and some of these (e.g. broad-band phase sihfting films) are similar to problems facing other applications in astronomical instruments (e.g. the FQPM coronagraph). These general arguments and analytic calculations appear sufficiently promising to justify more detailed modeling and experimentation.

We have presented some specific system design considerations associated with implementing a phase-contrast wavefront sensor into adaptive optics systems of current layout. It appears possible to "bootstrap" on the fly from a high-order Shack-Hartmann-based AO system, switching wavefront sensing and control to the phase-contrast sensor when an initial lock has reduced remnant phases below an acceptable level. It is hoped that such a switch would permit operation at Strehl ratios higher than 0.7, the approximate current limit at K = 2.2 um of the Palomar adaptive optics system, in view of apparently substantial sensitivity advantages enjoyed by the phase-contrast wavefront sensor.

ACKNOWLEDGMENTS

The research described in this publication was carried out at the Jet Propulsion Laboratory, California Institute of Technology, under a contract with the National Aeronautics and Space Administration.

REFERENCES

1. F. Zernike, "Das Phasenkontrastverfahren bei der Mikroskopischen beobachtung", *Z. Tech. Phys.,* Vol. **16**, p. 454, 1935
2. J. K. Wallace, "Summary of phase-contrast technique as applied to DM calibration for the PalAO Science Camera", JPL Memo, 10 October 2002
3. E. E. Bloemhof and J. A. Westphal, "Design Considerations for a Novel Phase-Contrast Adaptive-Optic Wavefront Sensor", *Proc. SPIE*, Vol. **4494**, pp. 363-370, 2002
4. E. E. Bloemhof and J. K. Wallace, "Phase contrast techniques for wavefront sensing and calibration in adaptive optics", *Proc. SPIE*, Vol. **5169**, pp. 309-320, 2003
5. P. Riaud, A. Boccaletti, D. Rouan, F. LeMarquis, and A. Labeyrie, "The Four-Quadrant Phase-Mask Coronagraph. II: Simulations", *Pub. Astronom. Soc. Pac.*, Vol. **113**, pp. 1145-1154, 2001
6. J. Goodman, "Introduction to Fourier Optics", McGraw-Hill, New York, 1968
7. M. Born and E. Wolf, "Principles of Optics", Pergamon Press, Oxford, UK, 1980
8. M. A. Vorontsov, E. W. Justh, and L. A. Beresnev, "Adaptive optics with advanced phase-contrast techniques. I. High-resolution wave-front sensing", *J. Opt. Soc. Am. A.*, Vol. **18**, No. 6, pp. 1289-1299, 2001
9. C. Roddier, F. Roddier, M. J. Northcott, J. E. Graves, and K. Jim, "Adaptive Optics Imaging of GG Tauri: Optical Detection of the Circumbinary Ring", *Ap. J.*, Vol. **463**, pp. 326-335, 1996
10. J. W. Hardy, "Adaptive Optics for Astronomical Telescopes", Oxford University Press, New York, NY, 1998

11. F. Roddier, C. Roddier, and N. Roddier, "Curvature sensing: a new wavefront sensing method", *Proc. SPIE*, Vol. **976**, pp. 203-209, 1988
12. R. G. Dekany, "The Palomar Adaptive Optics System", in *Adaptive Optics*, Vol. **13**, OSA Technical Digest Series (Optical Society of America, Washington, DC), pp. 40-42, 1996
13. M. Troy, R. G. Dekany, B. R. Oppenheimer, E. E. Bloemhof, T. Trinh, F. Dekens, F. Shi, T. L. Hayward, and B. Brandl, "Palomar Adaptive Optics Project: Status and Performance", *Proc. SPIE*, Vol. **4007**, pp. 31-40, 2000
14. D. L. Fried, "Least-square fitting a wave-front distortion estimate to an array of phase-difference measurements", *J. Opt. Soc. Am.*, Vol. **67**, No. 3, pp. 370-375, 1977
15. R. H. Hudgin, "Wave-front reconstruction for compensated imaging", *J. Opt. Soc. Am.*, Vol. **67**, No. 3, pp. 375-378, 1977
16. F. Shi, D. G. MacMartin, M. Troy, G. L. Brack, R. S. Burruss, and R. G. Dekany, "Sparse Matrix Wavefront Reconstruction: Simulations and Experiments", *Proc. SPIE*, Vol. **4839**, pp. 1035-1044, 2003
17. R. J. Sasiela, "Electromagnetic Wave Propagation in Turbulence", Springer-Verlag, Berlin, 1994
18. C. G. Wynne, "Extending the Bandwidth of Speckle Interferometry", *Opt. Commun.*, Vol. **28**, No. 1, pp. 21-25, 1979
19. C. Roddier, F. Roddier, F. Martin, A. Baranne, and R. Brun, "Twin-Image Holography with Spectrally Broad Light", *J. Opt. (Paris)*, Vol. **11**, No. 3, pp. 149-152, 1980
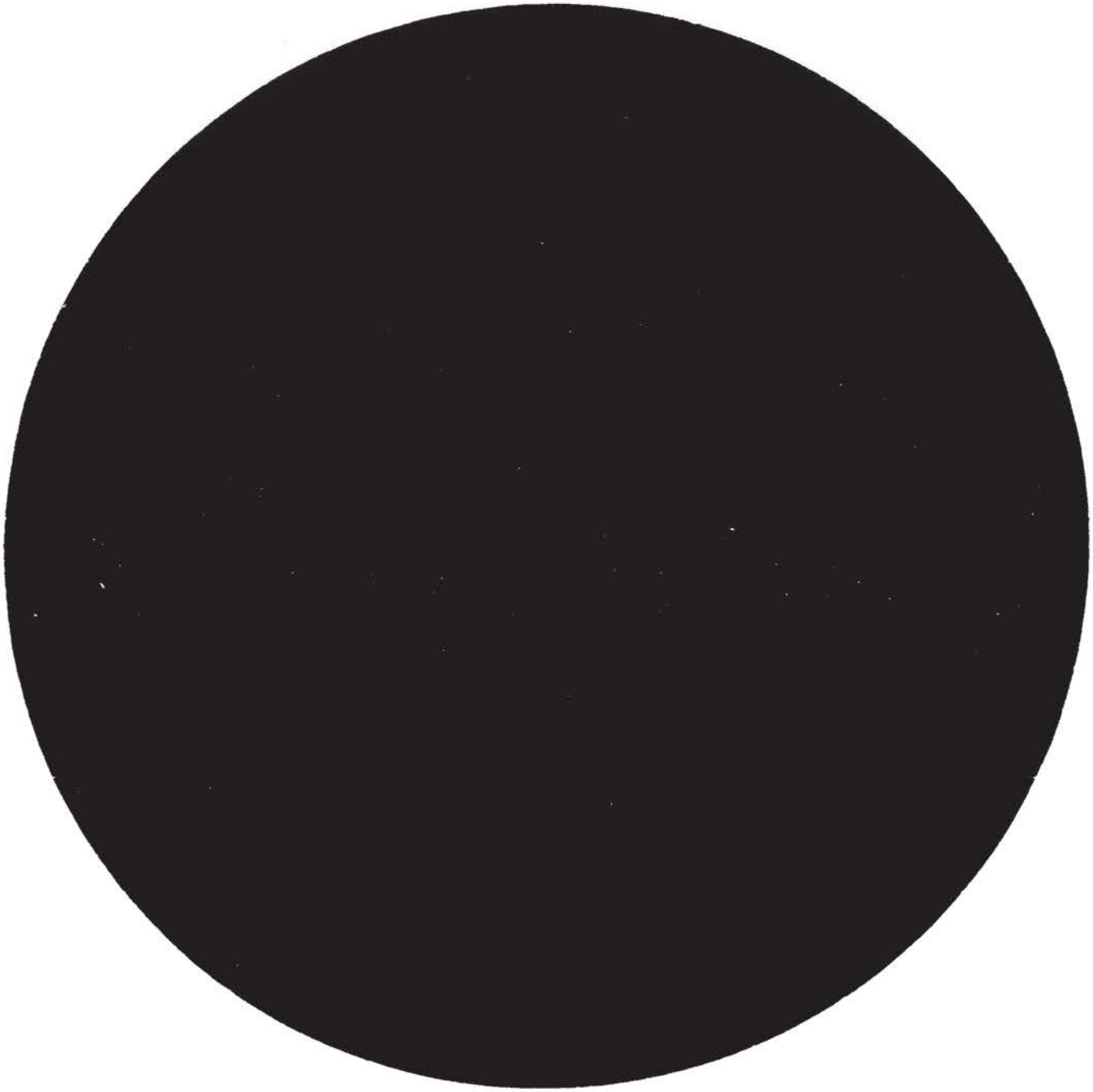
End of File